Interference of an Array of Independent Bose-Einstein Condensates

Zoran Hadzibabic, Sabine Stock, Baptiste Battelier, Vincent Bretin, and Jean Dalibard

Laboratoire Kastler Brossel, 24 rue Lhomond, 75005 Paris, France*

(Received 19 May 2004; published 26 October 2004)

We have observed high-contrast matter wave interference between 30 Bose-Einstein condensates with uncorrelated phases. Interferences were observed after the independent condensates were released from a one-dimensional optical lattice and allowed to overlap. This phenomenon is explained with a simple theoretical model, which generalizes the analysis of the interference of two condensates.

DOI: 10.1103/PhysRevLett.93.180403 PACS numbers: 03.75.Lm, 32.80.Pj

Studies of Bose-Einstein condensates (BECs) loaded into the periodic potential of an optical lattice have been continuously growing in the recent years [1]. These systems have a great potential for a range of applications such as modeling of solid state systems [2–6], preparation of low-dimensional quantum gases [7,8], tuning of atom properties [9,10], trapped atom interferometry [11,12], and quantum information processing [13,14].

One of the most commonly used probes of these novel systems are the interference patterns obtained when the gas is released from the lattice, so that the wave packets emanating from different lattice sites expand and overlap [3,11]. In particular, the appearance of high-contrast interference fringes in the resulting density distribution is commonly associated with the presence of phase coherence between different lattice sites.

In this Letter, we study the interference of a regular array of Bose-Einstein condensates with random relative phases. Independent condensates, each containing $\sim 10^4$ atoms, are produced in a one-dimensional (1D) optical lattice, in the regime where the rate of tunneling between the lattice sites is negligible on the time scale of the experiment. Contrary to what could be naively expected, we show that high-contrast interference fringes are commonly observed in this system. We present a theoretical model, which quantitatively reproduces our experimental results, and show that the periodicity of the lattice is sufficient for the emergence of a periodic atomic distribution after expansion, even in the absence of phase coherence between the condensates. This conclusion is independent of the dimensionality of the lattice. Our results generalize the study of the interference between two independent condensates [15–18]. In the last part of the Letter we briefly discuss the potential of our system for creating strongly number-squeezed states and report on an unexplained heating effect, which occurs for a narrow range of lattice depths.

Our experiments start with a quasipure ^{87}Rb condensate with 3×10^5 atoms in the $F = m_F = 2$ hyperfine state. Condensates are produced by radio frequency evaporation in a cylindrically symmetric magnetic trap. The harmonic trapping frequencies are $\omega_\perp/2\pi = 74$ Hz radially, and $\omega_z^{(0)}/2\pi = 11$ Hz axially, leading to cigar-shaped condensates with a Thomas-Fermi (TF) length of $L_{\mathrm{TF}} = 84$ μm, and a radius of $R_{\mathrm{TF}} = 6$ μm.

We then ramp up the periodic potential created by a 1D optical lattice. The lattice is superimposed on the magnetic trapping potential along the long axis (z) of the cigar [Fig. 1(a)]. Two equally polarized laser beams of wavelength $\lambda = 532$ nm intersect at an angle $\theta = 0.20$ rad to create a standing wave optical dipole potential with a period of $d = \lambda/[2\sin(\theta/2)] = 2.7$ μm. The two beams are focused to waists of about 100 μm, and carry a laser power of up to 220 mW each. The blue-detuned laser light creates a repulsive potential for the atoms, which accumulate at the nodes of the standing wave, with the radial confinement being provided by the magnetic potential. Along z, the lattice potential has the shape

$$V(z) = \frac{V_0}{2}\cos(2\pi z/d). \tag{1}$$

The lattice depth at full laser power is $V_0/h \approx 50$ kHz, and the number of occupied sites is $N = L_{\mathrm{TF}}/d \approx 30$.

Thanks to the long lattice period and the large height of the potential barrier between the sites, the 30 condensates can be completely isolated from each other. The matrix

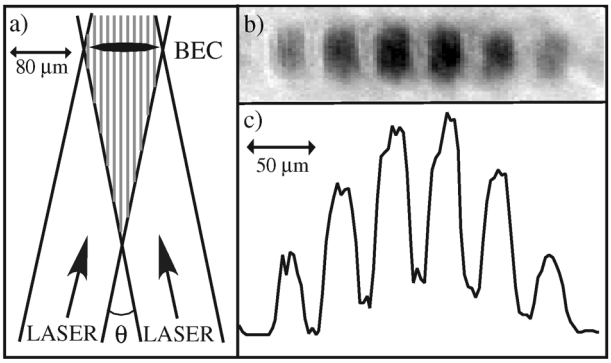

FIG. 1. Interference of Bose-Einstein condensates with uncorrelated phases. (a) A deep 1D optical lattice splits a cigar-shaped condensate into 30 independent BECs. (b) Absorption image of the cloud after 22 ms of expansion from the lattice. The density distribution shows clear interference fringes of high contrast. (c) Axial density profile of the cloud, radially averaged over the central 25 μm. The fit described in the text gives a fringe amplitude $A_1 = 0.64$ for this image.

element J for the tunneling between neighboring sites scales as $E_R e^{-2\sqrt{V_0/E_R}}$, where $E_R = \hbar^2 k^2/2m = h \times 80\,\mathrm{Hz}$, $k = \pi/d$, and m is the atom mass. For our maximum lattice depth of $V_0 \approx 600\ E_R$, and $n_0 \sim 10^4$ atoms per site, the Rabi frequency $n_0 J/h$ is less than 10^{-4} Hz and tunneling is negligible.

At full lattice depth, the gas at each site is in a quasi-two-dimensional regime. The motion along z is "frozen out" because the oscillation frequency $\omega_z/(2\pi)$ is 4 kHz, while the temperature and the chemical potential of the gas correspond to frequencies smaller than 2.5 kHz. Each condensate is therefore in the harmonic oscillator ground state along z, with a density distribution given by a Gaussian of width $\ell = \sqrt{\hbar/(2m\omega_z)} = 120\ \mathrm{nm} \ll d$.

In a typical experiment, we ramp up the lattice to $V_0 = 600\ E_R$ in $\tau_{\mathrm{ramp}} = 200$ ms. Initially, the chemical potential μ is constant across the system; different lattice sites contain different numbers of atoms, and the change in the interaction energy from site to site exactly compensates the change in the magnetic potential along z. As V_0 is ramped up, the cloud at each site gets more compressed, the interaction energy increases, and a continuous redistribution of particles is needed to maintain the uniformity of μ. Once tunneling becomes negligible ($V_0 \gtrsim 100\ E_R$), the occupation of different sites becomes fixed and further increase of V_0 leads to chemical potentials which differ from site to site. The independent evolution of each BEC then leads to dephasing of the various sites on a time scale of a few milliseconds (see below).

After holding the atoms in the lattice for another $\tau_{\mathrm{hold}} = 500$ ms, the optical and the magnetic trap are switched off simultaneously, and the density distribution of the cloud is recorded by absorption imaging after $t = 22$ ms of time-of-flight (TOF) expansion. Despite the fact that the phases of different BECs are completely uncorrelated, the images commonly show clear interference fringes. A spectacular example of this surprising phenomenon is given in Fig. 1(b) and 1(c) where the contrast is $>60\,\%$. Note that high-contrast interference is also observed if the lattice is ramped up on a thermal cloud with a temperature 3 times higher than the condensation temperature, so that the subsequently produced condensates "have never seen one another" [19].

We analyze the images by fitting the axial density profiles [Fig. 1(c)] with $[1 + A_1 \cos(B_1 + 2\pi z/D)]G(z)$, where $G(z)$ is a Gaussian envelope. This procedure extracts the first-harmonic modulation of the distribution, with the fitted period of 39 μm in agreement with the expected value $D = ht/(md)$. In Fig. 2(a), we summarize our results for 200 consecutively taken images. In most cases the fringe amplitude A_1 is significant, with mean value $\langle A_1 \rangle = 0.34$. The phase B_1 is randomly distributed between 0 and 2π. Consequently, no periodic modulation remains visible if we average the 200 density profiles.

In Fig. 2(b), we contrast this with the interference of 30 phase-correlated condensates. Here, we ramp up the lattice in $\tau_{\mathrm{ramp}} = 3$ ms and immediately release the BECs from the trap, before their phases completely diffuse away from each other. In this case, the fringe phases B_1 are clearly not randomly distributed, and the sum of 200 images still shows interference fringes of pronounced contrast. Phase correlations between the separated BECs were lost if the lattice was left on for $\tau_{\mathrm{hold}} \geq 3$ ms.

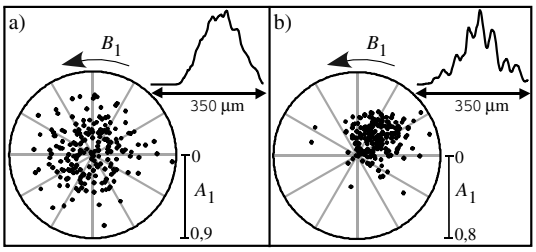

FIG. 2. Polar plots of the fringe amplitudes and phases (A_1, B_1) for 200 images obtained under the same experimental conditions. (a) Phase-uncorrelated condensates. (b) Phase-correlated condensates. Insets: Axial density profiles averaged over the 200 images.

We have numerically simulated our experiments with phase-uncorrelated condensates using the following model. We consider a 1D array of $N = 30$ BECs initially localized at positions $z_n = nd$ $(n = 1, \ldots, N)$, and assume that each condensate is in a coherent state described by an amplitude α_n and a phase ϕ_n [20]. We set $\alpha_n \propto n(N - n)$, corresponding to the Thomas-Fermi profile of the BEC at the point when the lattice is switched on. For expansion times $t \gg 1/\omega_z \approx 40\ \mu$s, the atom density at position z is given by [8]:

$$I(z) \propto \left| \sum_{n=1}^{N} \alpha_n e^{i\phi_n} e^{im(z-z_n)^2/(2\hbar t)} e^{-(z-z_n)^2/Z_0^2} \right|^2 \qquad (2)$$

where $Z_0 = \hbar t/(m\ell)$. We neglected the effects of the atomic interactions during the expansion. We perform a Monte Carlo analysis of $I(z)$ by assigning sets of random numbers to the phases $\{\phi_n\}$. We convolve the resulting density profiles with a Gaussian of 5 μm width to account for the finite resolution of our imaging system, and then fit them in the same way as the experimental data. The fitted fringe phase B_1 is randomly distributed between 0 and 2π. For the fringe amplitude we find $\langle A_1 \rangle^{\mathrm{sim}} = 0.31$, in excellent agreement with the experiment [21].

In order to give a more intuitive explanation of our observations, and generalize our analysis to arbitrarily large N, we make the following simplifications. We assume that all condensates contain the same average number of atoms, $\alpha_n = \alpha$, and that the expansion time t is large, so that $\ell, z_n \ll Z_0, \sqrt{\hbar t/m}$. In this case, Eq. (2) can be rewritten in the form $I(z) \propto N\alpha^2 e^{-2z^2/Z_0^2} F(z)$, where

$$F(z) = 1 + \sum_{n=1}^{N-1} A_n \cos(B_n + 2\pi n z/D) \qquad (3)$$

is a periodic function with period $D = ht/(md)$ and average value 1. $F(z)$ contains all the information about the contrast of the interference pattern. The amplitude A_n and the phase B_n of the n-th harmonic of $F(z)$ are given by the modulus and the argument of $(2/N)\sum_{j=n+1}^{N} e^{i(\phi_j - \phi_{j-n})}$.

If the N condensates have the same phase, $F(z)$ corresponds to the usual function describing the diffraction of a coherent wave on a grating

$$F(z) = \frac{1}{N}\frac{\sin^2(N\pi z/D)}{\sin^2(\pi z/D)}. \quad (4)$$

In this case, $F(z)$ has sharp peaks of height N and width $\sim 1/N$ at positions $z = pD$, where p is an integer. In between the peaks, $F(z) \sim 0$.

We now turn to the case of uncorrelated phases $\{\phi_n\}$. Using Monte Carlo sampling, we find for $10 \leq N \leq 10^4$:

$$\langle F_{\max}\rangle \sim 1.2\ln(N) \gg 1 \qquad \langle F_{\min}\rangle \sim \frac{0.2}{N} \ll 1 \quad (5)$$

where $F_{\max}$ and $F_{\min}$ are the maximum and the minimum "single-shot" values of $F(z)$, i.e., for a given set $\{\phi_n\}$. This shows that even for very large N, most single-shot $F(z)$ are strongly modulated. However, the width of the peaks of height $F_{\max}$ is $\sim 1/N$, and the fraction of the atoms contained in these peaks vanishes for $N \to \infty$.

We can recover the scaling laws of Eq. (5) by noticing that: (i) for large N, the probability distribution of F at any given point z is the same as for the laser intensity distribution for speckle, $p(F) = e^{-F}$, and (ii) the density distribution over an interval of length D consists of $\sim N$ independent values of F [22], so that the probability distributions for $F_{\max}$ and $F_{\min}$ are $Ne^{-F}(1 - e^{-F})^{N-1}$ and Ne^{-NF}, respectively.

The shape of $F(z)$ and the positions of its extrema vary randomly from shot to shot, and the density modulations can for most part be thought of as noise. In particular, the result $\langle F^2\rangle = 2\langle F\rangle^2$ (for $N \gg 1$) is characteristic of the Hanbury Brown and Twiss correlations for a fluctuating classical field. However, the underlying order of the lattice structure is sufficient to insure that this noise is strongly correlated [22], so that $F(z)$ is periodic with the same period D as in the coherent case.

The harmonic content of single-shot $F(z)$ is given by $C_n = \langle A_n^2\rangle = 4(N - n)/N^2$, each A_n resulting from summing $N - n$ complex numbers with random phases and moduli $2/N$. Note that $\sqrt{C_1} \approx 2/\sqrt{N} \approx 0.36$ for $N = 30$, which is close to the observed $\langle A_1\rangle$. The large modulation of $F(z)$ for $N \to \infty$ can be understood by noticing that while the weight of each harmonic decreases, their number increases [23]. It is interesting to contrast this with averaging N shots of two-condensate interference with an irreproducible phase [18]. In the latter case, the weight of the first harmonic is twice smaller and all the higher harmonics are absent, leading to a vanishing density modulation for large N.

We obtain similar results if we choose for the initial state a Mott insulator with exactly one atom per lattice site (see also [22]). In this case, the signal after TOF consists of the set of coordinates $\zeta_1, \ldots, \zeta_N$ where the N atoms are detected, and its harmonic content is given by:

$$C_n = \frac{4}{N(N-1)}\sum_{j=1}^{N}\sum_{j'\neq j}\langle e^{i2\pi(\zeta_j - \zeta_{j'})n/D}\rangle$$

where $\langle\ldots\rangle$ now denotes a quantum average. A simple calculation gives $C_{n\neq 0} = 4(N - n)/[N(N - 1)]$.

All of our arguments naturally extend into two and three dimensions (3D). In 3D, the function generalizing Eq. (3) is $F(\mathbf{r}) = 1 + \sum_{\mathbf{n}} A_{\mathbf{n}}\cos(B_{\mathbf{n}} + 2\pi\mathbf{n}\cdot\mathbf{r}/D)$ where $\mathbf{n} = (n_x, n_y, n_z)$ is a triplet of integers. This is a periodic function in x, y, z with a period D. In the experimental study of the superfluid to Mott insulator transition with cold atoms in 3D lattices [3,7], the disappearance of interference fringes is observed in the insulating domain, and used as one of the signatures for the loss of long range phase coherence. This seems in contradiction with our results. However one can reconcile the two findings by noticing that the experiments [3,7] are analyzed by integrating the density distribution $I(\mathbf{r})$ along the line of observation z. In this case, only the harmonics $(n_x, n_y, 0)$ are observed (see also [24]), which reduces the modulation amplitude by $\sqrt{N_z}$, where N_z is the number of sites along z. In fact, the effect is similar to that of averaging N_z images in a two-dimensional experiment [25].

In the next part of this Letter, we briefly discuss the potential of our setup for producing "number-squeezed" states with large occupation numbers [11], where the atom number on each site has a sub-Poissonian distribution with an average value $n_0 \gg 1$ and a standard deviation $\sigma < \sqrt{n_0}$. Such states are important for atom interferometry and precision measurements [28].

For simplicity, we restrict our discussion to the case of translational invariance, without the quadratic magnetic potential applied along the z axis. In the ground state of the system, the squeezing of the atom number on each site depends on the ratio of the tunneling rate $\tilde{t} = n_0 J/h$ and the effective strength of the repulsive on site interactions $U \sim \mu/n_0$, where μ is the chemical potential. To give a sense of scale, in our case $n_0 \sim 10^4$ and $U/h \sim 0.2$ Hz. We can qualitatively distinguish three regimes [11,29]: (i) For $J \geq n_0 U$, squeezing is negligible and the atom number on each site follows a Poissonian distribution ($\sigma = \sqrt{n_0} \sim 100$). (ii) For $J \sim U$ ($\tilde{t} \sim 200$ Hz), squeezing is significant and σ is reduced to $n_0^{1/4} \sim 10$. (iii) Finally, a phase transition to a Mott insulator state with $\sigma < 1$ occurs for $J \sim U/n_0$ ($\tilde{t} \sim 0.2$ Hz).

In our setup, we can tune the value of J across this full range, and the criterion for the Mott transition with $n_0 \sim 10^4$ atoms per site is satisfied for $V_0 \sim 100 - 150\,E_R$. However, we point out two practical difficulties which arise for such large values of n_0. First, for the system to be

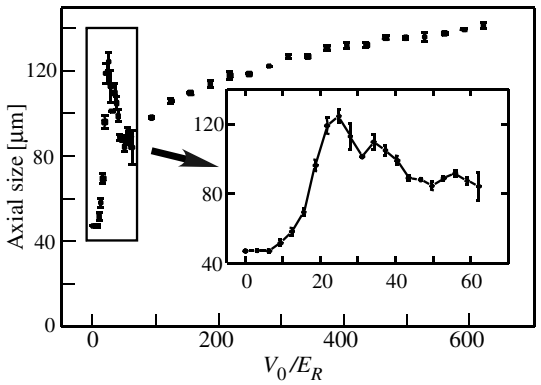

FIG. 3. Axial size of the cloud after 22 ms of expansion as a function of the lattice depth V_0. Inset: Zoom-in on the region where an unexplained heating of the cloud occurs. For all data points the lattice was raised in $\tau_{\mathrm{ramp}} = 200$ ms and left on for $\tau_{\mathrm{hold}} = 500$ ms before TOF. Error bars are statistical. Outside the heating region, the slow increase of the axial size matches the expected dependence $Z_0 \propto 1/\ell \propto V_0^{1/4}$.

in its ground state, all decoherence processes, such as particle loss, must have rates lower than $\tilde{t}$. Second, the assumed translational invariance must be insured to a sufficient level, so that the potential energies at different lattice sites match to better than $n_0 J = h\tilde{t}$. While it seems difficult to fulfill these criteria for the values of $\tilde{t}$ low enough for the Mott transition to occur, the regime of strong squeezing, $\sigma \lesssim n_0^{1/4}$, should be accessible.

In exploring the range of lattice depths 0–150 E_R, we have also observed an unexplained heating effect. For $20 < V_0/E_R < 45$ we observe strong heating of the system, which peaks for $V_0/E_R \approx 25$ and 35 (Fig. 3). The peak heating rate is $\sim$200 nK/s as long as the gas is at least partially condensed. However, once the condensate disappears, heating of the thermal cloud becomes negligible (< 10 nK/s). Outside $20 < V_0/E_R < 45$, heating due to the lattice is always negligible, independent of the lattice depth or the condensed fraction. We could not attribute this heating to any trivial technical effect, and it would be interesting to investigate further whether it is related to the onset of isolation and number squeezing of the BECs.

In conclusion, we have studied a 1D periodic array of independent condensates prepared in a deep optical lattice. We have shown that most single-shot realizations of this system show high-contrast interference patterns in a time-of-flight expansion. We have explained this effect with a simple model which naturally extends to 3D lattices. This initially surprising result should be taken into account in the ongoing studies of atomic superfluidity and coherence in optical lattices, where the contrast of the interference patterns is often used as a diagnostic.

We thank A. Browaeys, T. Esslinger, A. Georges, L. Pitaevskii, M. Kasevich, E. Altman, E. Demler, M. Lukin, and the ENS group for useful discussions. Z. H. acknowledges support from a Chateaubriand Grant, and S. S. from the Studienstiftung des deutschen Volkes, DAAD, and the Research Training Network Cold Quantum Gases HPRN-CT-2000-00125. This work is supported by CNRS, Collège de France, Région Ile de France, and DRED.

Note added.— Since the submission of this manuscript, two related theoretical papers have appeared [30,31].

*Unité de Recherche de l'Ecole normale supérieure et de l'Université Pierre et Marie Curie, associée au CNRS.

[1] I. Bloch, Phys. World **17**, 25 (2004).
[2] D. Jaksch *et al.*, Phys. Rev. Lett. **81**, 3108 (1998).
[3] M. Greiner *et al.*, Nature (London) **415**, 39 (2002).
[4] J. Hecker-Denschlag *et al.*, J. Phys. B **35**, 3095 (2002).
[5] F. S. Cataliotti *et al.*, Science **293**, 843 (2001).
[6] O. Morsch *et al.*, Phys. Rev. Lett. **87**, 140402 (2001).
[7] T. Stöferle *et al.*, Phys. Rev. Lett. **92**, 130403 (2004); M. Köhl *et al.*, cond-mat/0404338.
[8] P. Pedri *et al.*, Phys. Rev. Lett. **87**, 220401 (2001).
[9] B. Eiermann *et al.*, Phys. Rev. Lett. **92**, 230401 (2004).
[10] B. Paredes *et al.*, Nature (London) **429**, 277 (2004).
[11] C. Orzel *et al.*, Science **291**, 2386 (2001).
[12] Y. Shin *et al.*, Phys. Rev. Lett. **92**, 050405 (2004).
[13] S. Peil *et al.*, Phys. Rev. A **67**, 051603 (2003).
[14] H. Ott *et al.*, Phys. Rev. Lett. **93**, 120407 (2004)..
[15] J. Javanainen and S. M. Yoo, Phys. Rev. Lett. **76**, 161 (1996).
[16] M. Naraschewski *et al.*, Phys. Rev. A **54**, 2185 (1996).
[17] Y. Castin and J. Dalibard, Phys. Rev. A **55**, 4330 (1997).
[18] M. R. Andrews *et al.*, Science **275**, 637 (1997).
[19] P. W. Anderson, in *The Lesson of Quantum Theory*, edited by J. de Boer, E. Dal, and O. Ulfbeck (Elsevier, Amsterdam, 1986).
[20] This is equivalent to each condensate being in a Fock state, with the atom number following a Poisson distribution with a mean value α_n^2 (see, e.g., [17]).
[21] The unconvolved profiles give $\langle A_1 \rangle^{\mathrm{sim}} = 0.43$.
[22] E. Altman, E. Demler, and M. D. Lukin, Phys. Rev. A **70**, 013603 (2004).
[23] In practice, this means that a large modulation of $F(z)$ will be observed only if the imaging resolution is sufficient to detect a significant fraction of the harmonics.
[24] R. Bach and K. Rzążewski, Phys. Rev. Lett. **92**, 200401 (2004).
[25] We also stress that the effects discussed here differ from the low-contrast interference which can arise in the Mott regime due to inhomogeneity of the system [26] or incomplete isolation between the lattice sites [27].
[26] V. A. Kashurnikov, N. V. Prokof'ev, and B. V. Svistunov, Phys. Rev. A **66**, 031601(R) (2002).
[27] R. Roth and K. Burnett, Phys. Rev. A **67**, 031602(R) (2003).
[28] P. Bouyer and M. A. Kasevich, Phys. Rev. A **56**, R1083 (1997).
[29] W. Zwerger, J. Opt. B **5**, S9 (2003).
[30] R. Bach and K. Rzążewski, cond-mat/0407022.
[31] S. Ashhab, cond-mat/0407414.